Contrasting distribution of aggregates >100 μm in the upper kilometre of the South-Eastern Pacific

L. Guidi, G. Gorsky, Hervé Claustre, M. Picheral, L. Stemmann

HAL Id: hal-00330289
https://hal.science/hal-00330289

Submitted on 18 Jun 2008

Biogeosciences Discussions

Biogeosciences Discussions is the access reviewed discussion forum of *Biogeosciences*

Aggregates
distribution in the
South-Eastern Pacific

L. Guidi et al.

Printer-friendly Version

Interactive Discussion

EGU

Contrasting distribution of aggregates >100 μm in the upper kilometre of the South-Eastern Pacific

L. Guidi[1,2], G. Gorsky[1], H. Claustre[1], M. Picheral[1], and L. Stemmann[1]

[1]Université Pierre et Marie Curie-Paris 6, Laboratoire d'Océanographie de Villefranche;
CNRS, Laboratoire d'Océanographie de Villefranche, 06230 Villefranche-sur-Mer, France
[2]Department of Oceanography, Texas A&M University, College Station, TX 77843, USA

Correspondence to: G. Gorsky (gorsky@obs-vlfr.fr)

Abstract

Large sinking particles transport organic and inorganic matter into the deeper layers of the oceans. From 70 to 90% of the superficial particulate material is disaggregated within the upper 1000 m. This decrease with depth indicates that remineralization pro-
5 cesses are intense during sedimentation. Generally, the estimates of vertical flux rely on the sediment trap data but difficulties inherent in their design, limit the reliability of this information. During the BIOSOPE study in the southeastern Pacific, 76 vertical casts using the Underwater Video Profiler (UVP) and deployments of a limited number of drifting sediment traps provided an opportunity to fit the UVP data to sediment trap
10 flux measurements. We applied than the calculated UVP flux in the upper 1000 m to the whole 8000 km BIOSOPE transect. Comparison between the large particulate material (LPM) abundance and the estimated fluxes from both UVP and sediment traps showed different patterns in different regions. On the western end of the BIOSOPE section the standing stock of particles in the superficial layer was high but the export between 150
15 and 250 m was low. Below this layer the flux values increased. High values of about 30% of the calculated UVP maximum superficial flux were observed below 900 m at the HNLC station. The South Pacific Gyre exported about $2\,\mathrm{mg\,m^{-2}\,d^{-1}}$. While off Chilean coast 95% of the superficial matter was remineralized or advected in the upper kilometer, 20% of the superficial flux was observed below 900 m near the Chilean
20 coast. These results suggest that the export to deep waters is spatially heterogeneous and related to the different biotic and abiotic factors.

1 Introduction

The biological pump is the sum of biological processes by which atmospheric CO_2 fixed in photosynthesis is transferred from the euphotic layer to the ocean interior. Organic
25 and inorganic matter is transported into the deep layers mainly by sinking particles (Volk and Hoffert, 1985). Small (micrometers range) particles are considered to be

EGU

suspended material while large (>100 micrometers) particles are considered to settle. Size is an important parameter, determining among others the sinking velocity, mass content and food potential of particles. Particles volume distribution for surface water shows that most of the mass is encompassed in the 0.1–3 mm range (Jackson

5　et al., 1997). Stemmann et al. (2007) showed that the volume of large particles can equal the volume of the smaller ones. On the other hand, according to Richardson and Jackson (2007), picoplankton despite their small size, may contribute more to oceanic carbon export than currently recognized. Picoplankton can aggregate, be incorporated into settling detritus or consumed as aggregates or as individual cells by higher

10　trophic levels such as the pelagic filter-feeder tunicates or flux-feeder pteropods. This zooplankton short-circuit the microbial loop (Alldredge, 2005; Andersen et al., 1998; Gorsky et al., 1999; Noji et al., 1997) and transform small slowly settling particles into rapidly sinking large particulate matter (LPM). Organic particles leaving the euphotic zone sink until they are remineralized or reach the ocean bottom. Numerous studies

15　agree that relatively little of the organic matter that leaves the euphotic zone reaches the bottom. Particle flux at 1000 m is considered to be about 10% of that at 100 m (Betzer et al., 1984; Martin et al., 1987; Suess, 1980). The decrease in concentration of particles with depth (Bishop and Edmond, 1976; Gardner and Walsh, 1990) implies that intense solubilizing processes of sinking particles occur in the water column during

20　sedimentation. Particles can also be repackaged into larger faster settling objects with lower concentrations and therefore more difficult to sample.

Estimates of sinking material rely primarily on the deployment of sediment traps (Asper, 1987; Buesseler et al., 2007a; Gardner et al., 2000; Honjo et al., 1984). Problems associated with the use of sediment traps such as hydrodynamic flushing, swimmer

25　contamination, and sample degradation, make trap measurements difficult to validate (see Buessler et al., 2007, for review). According to Yu et al. (2001) the trapping efficiency of 40% is a typical minimum value for the pelagic upper ocean. One way to increase the reliability of quantitative estimations of vertical export of the particulate matter is to deploy neutrally buoyant traps which drifting in the sampled water mass

minimize the bias of advective effects (Buesseler et al., 2007a). In fact, most of the changes in flux with depth occur in the upper 1000 m (Lutz et al., 2002) and most of the processes that can bias flux estimates occur in this layer of the water column. On the other side, little attention is given in the literature to the role of the particle size distribution although many particle properties, fundamental in biogeochemical studies, such as sinking rate, carbon content depend on accurate determinations of particle size (Burd et al., 2007).

Here we are estimating the flux of particles by a method based on optical quantification of particles >100 μm (LPM) including the marine snow fraction (Gorsky et al., 2000; Guidi et al., 2007). As this methodology gives a detailed vertical assessment of the LPM abundance and size spectrum, we can estimate fluxes between the surface and the depth of 1000 m (the depth limit of the instrument's deployment)

The BIOSOPE (Biogeochemistry and Optics South Pacific Experiment) cruise covered a large range of contrasting hydrodynamic and trophic regimes along a ~8000 km transect from west of the Marquesas archipelago to the coastal waters of Chile (Claustre et al., 2008).

On the western end of the BIOSOPE transect, near Marquesas archipelago an enhancement of the primary production is visible from satellite. This level of production is often due to the island mass effect and has been explained by the dynamic interaction of the circulation and the topography (Martinez and Maamaatuaiahutapu, 2004, and references therein).

The South Pacific Gyre (SPG) is the largest subtropical anticyclonic gyre and the least described region of the ocean (Claustre and Maritorena, 2003; Longhurst, 1995). We know remarkably little about organic matter production and fate in it. The rare observations report very low chlorophyll concentrations (Chavez et al., 1995).

On the eastern end of the BIOSOPE transect large biomass is exported offshore and to the deep layers near the Chilean coast fuelled by the Chilean upwelling (Claustre et al., 2008; Thomas, 1999).

The Underwater Video Profiler (UVP see below for details) was used to assess the

EGU

particles stock and size spectrum at a high vertical resolution. As part of the BIOSOPE program we fitted the UVP data to sediment trap flux measurements and applied the UVP flux estimations to the 76 profiles made during the BIOSOPE transect. We characterised the distribution of the large particulate matter (LPM) and the resulting fluxes in the 1000 m water column over the whole transect.

2 Methods

2.1 Zone of the study and data acquisition

The BIOSOPE cruise was conducted from 26 October to 11 December 2004. The detailed description of the cruise including the sampling strategy is reviewed in Claustre et al. (2008).

Within this spatial context, we examined the vertical distribution of the Large Particulate Matter (LPM>100 μm to 2 cm) using a non-destructive imaging system the Underwater Video Profiler (UVP) constructed in the Laboratoire d'Océanologie of Villefranche sur mer, France. The vertical deployments were conducted from the surface to the depth of 1000 m (Table 1) at a descent speed of 1 m/s. During the section 76 vertical profiles were realised from Marquesas archipelago to the coastal waters of Chile (Fig. 1).

The UVP coupled to a CTD SBE19 (Seabird Inc.) quantified and measured objects illuminated in a slab of water of known volume of 10.53 L. Object sizes are represented by the number of pixels in an image. Size and volume calibrations were conducted in a sea-water tank using natural particles of different types to determine the conversion between pixels to metric units (Stemmann et al., 2002). Images were recorded digitally at a rate of 12 images per second and processed with custom made image analysis software (Gorsky et al., 2000). The equivalent spherical diameter (ESD) of each particle was calculated assuming that the particle projected shape was a circle.

The resulting particles size distribution and flux data integrated over 5 m intervals

were related to the simultaneously acquired CTD and fluorescence data.

2.2 Flux estimation from the size spectrum of particles

The mass flux was calculated from size spectra using the method from Guidi et al. (2008)[1].

The mass of a spherical particle with diameter (d) is given by

$$m(d) = \alpha \, d^3 \tag{1}$$

where $\alpha = \pi \, \rho/6$ and ρ is its average density.

Its settling rate can be calculated using Stokes Law:

$$w(d) = \beta \, d^2 \tag{2}$$

where $\beta = g \, (\rho - \rho_0)(18\upsilon\rho_0)^{-1}$, g is gravitational acceleration, ρ_0 is the fluid density, and υ is the kinematic viscosity.

The size spectrum of a "population" of particles is usually defined in terms of the number concentration of particle (ΔC) in a given small size range (Δd): $n = \Delta C / \Delta d$. The total mass flux (F_p) is the mass flux integrated over all particle sizes. Using diameter (d) as a measure of particle size, then:

$$F_p = \int_0^\infty n(d)m(d)w(d)\mathrm{d}d \tag{3}$$

Aggregate flux (F_p) is equal to aggregate mass multiplied by aggregate settling rate (Eq. 3). Hence, with some simplification aggregate mass flux can be related to ag-

---

[1]Guidi, L., Jackson, G. A., Stemmann, L. Miquel, J. C., Picheral, M., and Gorsky, G.: Particle size distribution and flux in the mesopelagic: a close relationship, Deep-Sea Res. I., in revision, 2008.

Aggregates distribution in the South-Eastern Pacific

L. Guidi et al.

EGU

gregate size by power relationship (Eq. 1 and Eq. 2; Alldrege and Gotshalk, 1988; McCave, 1984; Alldredge, 1998) following:

$$F_p = \sum_{i=1}^{m} n_i \cdot A \cdot d_i^b \tag{4}$$

Note that the flux integration is only for particles between classes i to m available with the UVP, not the $0-\infty$ shown in Eq. (3).

Hence, knowing A and b (Eq. 4), aggregate with a given size (d) can be directly related to its mass flux. Estimated fluxes with UVP were compared to matching sediment trap observations at global scale. A minimization procedure using the Matlab function *fminsearch* (Mathworks Inc., Natick, MA) provided a means to calculate A and b providing the best fit between the two fluxes, measured from sediment traps and estimated from particle size distributions (Guidi et al., 2008[1]). Residues' normality between model (estimated UVP flux) and data (sediment traps) were tested and the model validated.

Finally different relationships were described between mass, fluxes of organic and inorganic carbon and, particulate nitrogen and aggregate size distributions. The mass flux is given in units of dry weight (DW).

3 Results

3.1 Hydrology

The general hydrology studied during the BIOSOPE cruise is described in Claustre et al. (2008). The surface salinity pattern varied over a large range, from the highly salty waters associated with the South Pacific Tropical Waters (SPTW) around 130° W (salinity of 36.6) towards the Eastern South Pacific Intermediate Water (ESPIW), at 78° W (salinity of ~34, Fig. 1). The South Equatorial Current (SEC) surrounding the Marquesas Islands (stations MAR) constituted the southern border of High Nutrients

Low Chlorophyll (HNLC) waters of the equatorial upwelling region (see Claustre et al., 2008, and the references herein). The South Pacific gyre (station GYR) was characterized by the strongly stratified Eastern South Pacific Central Waters (ESPCW). East of 100° W, the transition zone between the ESPCW and the waters, influenced by fresher Subantarctic Surface Waters (SASW, Fig. 1), marked the subtropical front. East of EGY stations a tongue of low salinity waters was observed at a depth of 300 m and flowed close to the surface near the coast.

East of 78° W, the ESPIW lies above the relatively saltier Equatorial Subsurface Water (EESW), which extends in the 100–400 m range. The ESPIW is part of the poleward Peru-Chile undercurrent (PCUC, stations UPW, UPX).

3.2 Distribution of the biogeochemical parameters

The distribution and amounts of total chlorophyll a concentration (TChl$a$) measured along the transect by different methods were similar (Raimbault et al., 2007 and Ras et al., 2007). These in situ chlorophyll a measurements matched the values derived from satellite imagery and showed considerable variations along the section. The highest concentrations of TChl$a$ were recorded in surface layers at the western and eastern extremities; very low chlorophyll content was measured in the center of the SPG. The lowest concentration occurred near the surface at 114° W ($\sim$0.02 mg TChl$a$ m^{-3}). Distribution of the in vivo fluorescence of TChl$a$ (Fig. 2) shows the range of variation of the autotrophic biomass along transect.

The water column was explored in more detail during the long stations (Fig. 3). Drifting sediment traps were deployed below the mixed layer (Claustre et al., 2008).

During the BIOSOPE cruise, the subsuperficial LPM distribution was generally correlated with the vertical distribution of fluorescence (Fig. 3) suggesting a direct relationship between the two parameters. Except the UPX station near the Chilean coast, this relationship was not evident in the deeper layers where the UVP maxima were certainly associated with the detritic or heterotrophic matter. LPM biovolume and abundance were the lowest respectively at the GYR, EGY and HNLC stations while near Chile the

EGU

water column contained the highest volumes of LPM (Figs. 3 and 4). However, considering only the euphotic zone (see Claustre et al., 2008) the MAR and UPW stations displayed the highest maximum LPM values.

3.3 Comparison of the distinct zones along the BIOSOPE transect

LPM concentrations along the BIOSOPE transect (Fig. 4) reveal the following features: 1) high abundance of particles in the superficial layer at the station MAR and relatively high concentration of particles from 150–300 m. 2) deep LPM maximum between 135 and 130° W, 3) a discontinuity in the abundance pattern at the vicinity of 100° W and 4) low particle densities in the low salinity ESPIW water mass (Figs. 1 and 4).

3.3.1 Western portion of the section

The mass flux estimated from size distribution profiles of the LPM along the BIOSOPE transect revealed a strong potential export in the superficial 150 m at the western end of the transect (Fig. 5). However, below this layer, between 150 and 300 m at the MAR station the LPM vertical flux was very low, forming a discontinuity stratum between the surface and the mesopelagic layers (Fig. 5). Despite the low vertical fluxes at this station (Fig. 5) the abundance of particles was high (Fig. 4). This observation may be explained by the small size and low settling velocities of these particles. The section between MAR and GYR is characterized by the increasing oligotrophy and by the deepening of the nutricline (Raimbault et al., 2007). The deep chlorophyll maximum (DCM) deepens also (Figs. 2 and 3), its base follows the 26 kg m^{-3} isopycnal (Claustre et al., 2008).

3.3.2 The South Pacific gyre

As expected the lowest values of particles abundance and the lowest export values were measured in and below the GYR. Abundances were higher in the 100–400 m layer. The low biovolume and low fluxes indicate that particles in the SPG were small

Aggregates distribution in the South-Eastern Pacific

L. Guidi et al.

EGU

(Figs. 3 and 5). Eastwards, the strong salinity gradient delineated the limit of the SPG and indicated the presence of the subtropical frontal zone (Fig. 1). A discontinuity in the particle abundance pattern was observed in this zone and the vertical fluxes displayed the lowest values.

3.4 Eastern portion of the section

East of the EGY station, and below the ESPIW waters (at a depth of 250 m and below) the water mass had small particle abundance and low vertical flux values. A significant decrease in the concentration of particles was observed at the UPW station in the subsurface layer. Nevertheless, the particulate volume and vertical export remained high. This result suggests that the contribution of large size class particles in the particles population was high. Near the Chilean coast the mixed layer was reduced and the nutrient concentrations and the primary production were high. At the UPX station the Chl*a* fluorescence signal was measurable even in the intermediate layers. The abundance of particles and the resulting vertical flux was high in the entire water column (Figs. 4 and 5).

4 Discussion

Marine particles vary in length from submicron colloidal particles to marine snow larger than tens of millimeter in diameter (Alldredge and Gotschalk, 1988; Fowler et al., 1987). The concentration of particles varies across this size range, with smaller particles generally being more abundant than larger ones (McCave, 1975). The particle mass however, tends to be concentrated in the larger particles (e.g., Jackson et al., 1997; McCave, 1975).

During the BIOSOPE cruise several contrasting provinces (from oligotrophy to eutrophy) were studied using the Underwater Video Profiler (UVP). This instrument was built for exhaustive optical estimation of 1) the stock of the particles >100 μm (large particu-

late matter – LPM) from the surface to the depth of 1000 m and 2) their size distribution (Stemmann et al., 2007). We estimated the LPM mass flux along the whole transect. Drifting sediment traps (Claustre et al., 2008) were deployed during the long stations below the mixed layer (between 200 and 400 m depth range). We could therefore com-
5   pare the UVP estimations with the biomass collected in the traps. As described more in details in Guidi et al. (2008)[1], we integrated the mass flux over all the particles according to their sizes. We used particle diameter to estimate their mass and their settling rate (see Methods section). A minimization procedure was applied to find the best fit between the two fluxes on a global scale. Flux estimations were made for the 76 UVP
10   profiles made during the cruise and were compared to the drifting sediment traps mass flux measurements (Fig. 6).

Fluxes can be calculated from size spectrums as showed above and the results fitted to sediment trap measurements (Fig. 6). This procedure allows for a comparison of fluxes in the 1000 m water column sampled by the UVP. When fitting the UVP data to
15   free-drifting trap data we assumed that the latter are correct. Thus we do not improve the sediment trap measurements but as the correlation between the optical assessment and the collected matter is good we are applying the flux estimations to all the 76 UVP profiles providing extensive information on the potential vertical export in the different depths along the whole transect. Image acquisition is a conservative sam-
20   pling method. With the improvement of the sediment trap methodology sensu Buesseler et al. (2007b) we will be able to ameliorate also the traps-UVP correlations and provide more precise flux data with high spatial and temporal resolution. This treatment can be done retrospectively and also on past data stored in the UVP databank (http://www.obs-vlfr.fr/LOV/ZooPart/UVP/).

EGU

4.1 Abundance vs. fluxes

4.1.1 Western portion of the section

On the western end of the BIOSOPE transect, (station MAR), the abundance of particulate matter in the superficial layer is very high (Fig. 4). According to Gomez (2007), the small pennate cluster forming diatom *Pseudo-nitzschia delicatissima* and the large centric diatom *Rhizosolenia bergonii* were the main microphytoplanktonic constituents of this layer. Large, rapidly sinking phytoplankton, such as diatoms, are believed to control carbon flux from upper ocean layers (Michaels and Silver, 1988). However as pointed out by Gomez (2007) in the western and eastern part of the BIOSOPE transect the superficial diatom population was characterized by frustules with low silicate content because of the silicate-limited environment. This feature may limit also their ballasting efficiency.

Although the abundance profile shows a vertical continuum and the surface LPM maximum is the second highest on the whole transect (Fig. 4), the flux estimations calculated from the UVP data fitted to the drifting sediment trap measurements reveal that the export between 150 and 250 m is very low (Fig. 5). This discontinuity in the vertical flux clearly observed at the station MAR may be the result of different biological and physical factors. Large unknown transparent objects were detected by the UVP at the MAR site (see Fig. 7 in Stemmann et al., 2007). These circular-shaped objects were about 2–5 mm in diameter with concentrations between 1–10 objects L^{-1}. They were located throughout the upper 200 m but below 170 m their concentration decreased. They might increase the potential flux values in the superficial layer. Below this layer the population was composed of small particles. The hydrology at the MAR site may also contribute to the discontinuity in the vertical export. The discontinuity stratum (150–250 m) corresponds to the zone of narrowing density field and is the site of strong advective processes (Figs. 3 and 4 in Claustre et al., 2008). These advective processes may be responsible of the change in the size structure of the particles population. Below this discontinuity layer the vertical flux values increase. This feature is

EGU

clearly visible in the Fig. 7.

An increase of the LPM flux was observed in the HNLC zone in the vicinity of 130° W. This increase may be associated with the deepening of the sub-surface isotherms (Claustre et al., 2008). About 30% of the maximum superficial flux was observed below 900 m at the HNLC station. In fact, the mean export initially decreased at 200 m when compared to the maximum flux at the surface layer, but than it increased with depth (Fig. 3 and 7). The superficial production at this region is weak. Only about 99 mg m^{-2} d^{-1} in the maximum layer but still about 20 mg m^{-2} d^{-1} below 900 m. The reason of the deep increase of the exported mass may be linked among other processes to the aggregation, advection or to the anoxic conditions. Furthermore, no significant difference was observed between the day and night fluxes that may be attributed to the vertical zooplankton migration (Stemmann et al., 2007) and according to Claustre et al. (2008) in this area the currents were weak. Therefore, the hypothesis that the increase of large particles flux may be associated with suboxic conditions should be further explored. According to Claustre et al. (2008) this oxygen minimum reflects the signature of a north-westwards propagation of the oxygen minimum zone developed along South America. The suboxic conditions might prevent the degradation of particulate matter This hypothetical particle preservation could also occur in the Marquesas area. Below 200 m there is a good conservation of the mass flux. Mass flux estimated at 900 m corresponds to 70% of mass flux estimated at 200 m.

4.1.2 The South Pacific gyre

The SPG is known as a hyper-oligotrophic water mass (Claustre and Maritorena, 2003; Morel et al., 2007). The biological production in the superficial layer is the lowest in the global ocean. Peaks of small particles centered at 100 m were associated with a *Prochlorococcus* sp. population (Grob et al., 2007). The deep chlorophyll maximum (DCM) located between 160–200 m was mainly composed of pico-phytoeukaryotes, although some coccolithophorid and diatom cells were also present (Beaufort et al., 2007; Gomez et al., 2007; Ras et al., 2007). The maximum phaeophorbide (a tracer for

Aggregates distribution in the South-Eastern Pacific

L. Guidi et al.

EGU

altered Chl*a*) concentration was found also in this layer (Ras et al., 2007). Oligotrophic regions, where small cells dominate the production, can contribute significantly to the global carbon flux via detritus (Richardson and Jackson, 2007). The mass flux associated with the DCM was estimated from the UVP data as ~30 mg m^{-2} d^{-1}. 20% of this flux was estimated to be exported below 200 m and about 8% below 900 m (~2 mg m^{-2} d^{-1}). While considering the large geographical extent of the SPG, this extreme oligotrophic ecosystem is producing a non negligible amount of carbon. Due to the lack of seasonal vertical mixing and weak lateral advection, the biologically produced LPM carbon can be exported and trapped in the deep layers for long periods.

4.1.3 Eastern portion of the section

In the vicinity of 100° W, we are observing a clear discontinuity in the abundance distribution of the LPM (arrow in Fig. 4). This discontinuity corresponds to the uplifted isolines delineating the subtropical front as described in Claustre et al. (2008). At EGY, the DCM is located at the depth of 80 m but the export values are low, similar to the HNLC station. The mean superficial maximum export is estimated as 127 mg m^{-2} d^{-1}, and a slight increase of fluxes with depth can be observed (Fig. 7). About 13% of the superficial export is measured below 900 m. This result constitutes 94% of the vertical flux estimated at 200 m. No difference was observed between the day and night fluxes.

The situation is contrasting off and near Chilean coast. High LPM concentrations are observed at the superficial layer with a strong decrease below this layer at the location of the low salinity waters (Fig. 1). This feature is not detected on the flux plot (Fig. 5). Therefore, the decrease in abundance is related to the small particle fraction. At the UPW station, the situation is different. The potential export from the Chl*a* maximum estimated for the whole section is 7367 mg m^{-2} d^{-1}. At the depths of 200 m only 4.6% and below 900 m only 1.5% of this flux remained. Thus, 95% of the matter was remineralized or advected. At both coastal stations the vertical zooplankton migration was significant. Near the Chilean coast, at the UPX stations, the vertical flux remained high in the entire water column. The surface maximum export was 1400 mg m^{-2} d^{-1}, lower

EGU

than the mean UPW surface maximum but in contrary to the latter, 20% of the superficial flux was observed below 900 m (Fig. 7). Thus the remineralization processes differ in the two stations near the Chilean coast.

4.2 Export efficiency

Particulate export is a result of particle supply, production, consumption and aggregation. These processes are developed at different scales of variability including time lags between biological production and export. During settling, particles disaggregate, decompose and disappear. Most are transformed into smaller particles or into dissolved matter by the processes of remineralization. Some may coalesce into larger particles by grazing or aggregation (Alldredge and Silver, 1988; Jackson and Burd, 2002). It is at depths between the surface euphotic zone and roughly 1000 m where most sinking particles are remineralized (Buesseler et al., 2007b). The variety of vertical profiles shows that there are variations in remineralization rates or advection rates with depth. Blooms of some species, like coccolithophores or diatoms and the consequent phytodetritus deposition, can cause episodic changes in remineralization length-scales (Nodder et al., 2007); blooms of filter-feeder thaliaceans, larvaceans or flux-feeder pteropods can change element ratios, sinking speeds and ballasting (Alldredge, 2005; Andersen et al., 1998; Boyd and Newton, 1995) or size distributions of particles (Gorsky et al., 1999). Zooplankton affect particle flux in the sea in a number of ways; they create or aggregate particles by feeding and producing sinking fecal pellets, disaggregate sinking particles by their feeding or swimming activities, remineralize sinking particles through their feeding and metabolism, and actively transport particulate and dissolved organic matter from the surface to depth by vertical migration (e.g., Fowler et al., 1987; Longhurst et al., 1990). Beyond the overall changes in particle flux with depth, changes in composition of the sinking material can have an impact on carbon gradients. Steinberg et al. (2008), compared losses of sinking POC measured by neutrally buoyant sediment traps with bacteria and zooplankton metabolic requirements in the subtropical Pacific and in the subarctic Pacific. Mesopelagic bacterial carbon demand was

Aggregates distribution in the South-Eastern Pacific

L. Guidi et al.

EGU

respectively 3- to 4-fold, and 10 fold greater than the loss of sinking POC flux, while zooplankton carbon demand was 1- to 2 fold, and 3- to 9-fold greater. Nevertheless, on the studied section and in the different trophic regimes UVP data indicate that particle export below 900 m was not negligible.

During the BIOSOPE transect in the different geographic zones the relative fluxes when compared to the superficial maximum were different (Fig. 8). Higher proportion of particulate matter was mediated to the deep layers in the GYR region than in the superficially rich MAR or UPW zones.

Sinking velocities determine the depth at which remineralization occurs, which in turn determines how soon remineralized nutrients and carbon will be returned to the surface ocean (Sarmiento and Gruber, 2006). Particles of the same excess density settle at roughly the same speed principally because Reynolds number is very sensitive to particle size (Khelifa and Hill, 2006a, b). Although organic compounds are initially present in different proportions in the particles with different settling velocities, the degradation process can lead to uniform chemical compositions of particles (Goutx et al., 2007). This change reflects the processes of loss through enzymatic hydrolysis of source compounds and input of bacterial biomass. The settling speed may differ in the different regions due to the differences in the composition of primary and secondary producers. More studies should test the hypothesis on which our flux estimations are based, i.e., that at mesopelagic depths particles of similar size settle at a more or less uniform speed due to their similar composition.

5 Conclusions

Stock and size spectrum of particles >100 μm was optically estimated from the surface to the depth of 1000 m and the mass flux of the particle bulk calculated. The resulting mass fluxes estimated with the UVP were compared to the drifting sediment trap data and applied over the whole BIOSOPE transect.

The LPM abundance and the estimated fluxes differed within the study area. At the

EGU

MAR station the abundance profile showed a vertical continuum while the vertical flux decreased significantly between 150 and 250 m. This change could be due to circular-shaped objects 2–5 mm in diameter with concentrations between 1–10 objects L^{-1} observed in the superficial layer, as well to intense hydrodynamic processes (Figs. 3 and 4 in Claustre et al., 2008) in this zone. Only about 2% of the superficial LPM was exported below 900 m.

Contrastingly, about 30% of the maximum superficial flux was observed below 900 m at the HNLC station. This feature may be associated to the suboxic (Claustre et al., 2008) conditions.

In spite of relatively small values (2% of the superficial maximum), the carbon export below the extreme oligotrophic SPG is not negligible. The lack of seasonal vertical mixing and weak lateral advection suggest that this matter can be trapped in the deep layers for long periods.

A discontinuity in the abundance distribution of the LPM is observed in the vicinity of 100° W and is associated with the intrusion of the subtropical front.

High LPM concentrations are observed in the superficial layer off and near Chilean coast. There is a strong decrease of particles abundance below this layer in the low salinity waters, but not in the vertical flux, suggesting a decrease in the small particles population only.

The potential export from the Chl*a* maximum displays the highest value at the UPW station but at the depths of 200 m only 4.6% and below 900 m only 1.5% of this flux remains. 95% of the matter is remineralised or advected above 200 m.

At the UPX station, the vertical flux remains high in the entire water column. In contrast to UPW, 20% of the superficial flux is still observed below 900 m.

Variations in the estimated flux rates of LPM obtained in this study suggest that a wide variety of biotic and abiotic processes may drive the aggregation-disaggregation processes and influence the export of matter from mesopelagic layers. This conclusion suggests that LPM export to deep waters is heterogeneous and that optical methods allowing high spatial resolution studies should be utilized in deep sea habitats.

EGU

References

Alldredge, A.: The contribution of discarded appendicularian houses to the flux of particulate organic carbon from oceanic surface waters, in: Response of marine ecosystems to global change: Ecological impact of appendicularians, edited by: Gorsky, G., GB Science Publishers-Editions Scientifiques GB, Paris, 309–326, 2005.

Alldredge, A. L. and Gotschalk, C.: In situ settling behavior of marine snow, Limnol. Oceanogr., 33, 339–351, 1988.

Alldredge, A. L. and Silver, M. W.: Characteristics, dynamics and significance of marine snow, Prog. Oceanogr., 20, 41–82, 1988.

Andersen, V., Francois, F., Sardou, J., Picheral, M., Scotto, M., and Nival, P.: Vertical distributions of macroplankton and micronekton in the ligurian and tyrrhenian seas (northwestern mediterranean), Oceanol. Acta, 21, 655–676, 1998.

Asper, V. L.: Measuring the flux and sinking speed of marine snow aggregates, Deep-Sea Res. I, 34, 1–17, 1987.

Beaufort, L., Couapel, M., Buchet, N., and Claustre, H.: Calcite production by Coccolithophores in the South East Pacific Ocean: from desert to jungle, Biogeosciences Discuss., 4, 3267–3299, 2007,
http://www.biogeosciences-discuss.net/4/3267/2007/.

Betzer, P. R., Showers, W. J., Laws, E. A., Winn, C. D., Ditullio, G. R., and Kroopnick, P. M.: Primary productivity and particle fluxes on a transect of the equator at 153-degrees-w in the pacific-ocean, Deep-Sea Res. I, 31, 1–11, 1984.

Bishop, J. K. B. and Edmond, J. M.: A new large volume filtration system for the sampling of oceanic particulate matter, J. Mar. Res., 34, 181–198, 1976.

Boyd, P. and Newton, P.: Evidence of the potential influence of planktonic community structure on the interannual variability of particulate organic-carbon flux, Deep-Sea Res. I, 42, 619–639, 1995.

BGD

5, 871–901, 2008

Aggregates distribution in the South-Eastern Pacific

L. Guidi et al.

Title Page

Abstract	Introduction
Conclusions	References
Tables	Figures

◄ ►|

◄ ►

Back | Close

Full Screen / Esc

Printer-friendly Version

Interactive Discussion

EGU

Buesseler, K. O., Antia, A. N., Chen, M., Fowler, S. W., Gardner, W. D., Gustafsson, O., Harada, K., Michaels, A. F., van der Loeff, M. R., Sarin, M., Steinberg, D. K., and Trull, T.: An assessment of the use of sediment traps for estimating upper ocean particle fluxes, J. Mar. Res., 65, 345–416, 2007a.

Buesseler, K. O., Lamborg, C. H., Boyd, P. W., Lam, P. J., Trull, T. W., Bidigare, R. R., Bishop, J. K. B., Casciotti, K. L., Dehairs, F., Elskens, M., Honda, M., Karl, D. M., Siegel, D. A., Silver, M. W., Steinberg, D. K., Valdes, J., Van Mooy, B., and Wilson, S.: Revisiting carbon flux through the ocean's twilight zone, Science, 316, 567–570, doi:10.1126/science.1137959, 2007b.

Burd, A. B., Jackson, G. A., and Moran, S. B.: The role of the particle size spectrum in estimating poc fluxes from 234th/238u disequilibrium, Deep-Sea Res. I, 54, 897–918, 2007.

Chavez, F. P., Buck, K. R., Bidigare, R. R., Karl, D. M., Hebel, D., Latasa, M., Campbell, L., and Newton, J.: On the chlorophyll-a retention properties of glass-fiber gf/f filters, Limnol. Oceanogr., 40, 428–433, 1995.

Claustre, H. and Maritorena, S.: The many shades of ocean blue, Science, 302, 1514–1515, 2003.

Claustre, H., Sciandra, A., and Vaulot, D.: Introduction to the special section: bio-optical and biogeochemical conditions in the South East Pacific in late 2004 – the BIOSOPE cruise, Biogeosciences Discuss., in press, 2008.

Fowler, S. W., Buat-Menard, P., Yokoyama, Y., Ballestra, S., Holm, E., and Van Nguyen, H.: Rapid removal of chernobyl fallout from mediterranean surface waters by biological activity, Nature, 329, 56–58, 1987.

Gardner, W. D. and Walsh, I. D.: Distribution of macroaggregates and fine-grained particles across a continental-margin and their potential role in fluxes, Deep-Sea Res. I, 37, 401–411, 1990.

Gardner, W. D., Richardson, M. J., and Smith, W. O.: Seasonal patterns of water column particulate organic carbon and fluxes in the ross sea, antarctica, Deep-Sea Res. II, 47, 3423–3449, 2000.

Gomez, F.: On the consortium of the tintinnid eutintinnus and the diatom chaetoceros in the Pacific ocean, Mar. Biol., 151, 1899–1906, 2007.

Gorsky, G., Chretiennot-Dinet, M. J., Blanchot, J., and Palazzoli, I.: Picoplankton and nanoplankton aggregation by appendicularians: Fecal pellet contents of megalocercus huxleyi in the equatorial pacific, J. Geophys. Res.-Oceans., 104, 3381–3390, 1999.

Gorsky, G., Picheral, M., and Stemmann, L.: Use of the underwater video profiler for the study

EGU

of aggregate dynamics in the north mediterranean, Estuar. Coast. Shelf Sci., 50, 121–128, 2000.

Goutx, M., Moriceau, B., Lee, C., Liu, Z., Guigue, C., Duflos, M., Tedetti, M., Sempere, R., Wakeham, S. G., and Xue, J.: Composition and degradation of marine particles with different settling velocities, Limnol. Oceanogr., 52(4), 1645–1664, 2007 .

Grob, C., Ulloa, O., Claustre, H., Huot, Y., Alarcón, G., and Marie, D.: Contribution of picoplankton to the total particulate organic carbon (POC) concentration in the eastern South Pacific, Biogeosciences, 4, 837–852, 2007, http://www.biogeosciences.net/4/837/2007/.

Guidi, L., Stemmann, L., Legendre, L., Picheral, M., Prieur, L., and Gorsky, G.: Vertical distribution of aggregates ($>110\,\mu m$) and mesoscale activity in the northeastern atlantic: Effects on the deep vertical export of surface carbon, Limnol. Oceanogr., 52, 7–18, 2007.

Honjo, S., Doherty, K. W., Agrawal, Y. C., and Asper, V. L.: Direct optical assessment of large amorphous aggregates (marine snow) in the deep ocean, Deep-Sea Res. I, 31, 67–76, 1984.

Jackson, G. A., Maffione, R., Costello, D. K., Alldredge, A. L., Logan, B. E., and Dam, H. G.: Particle size spectra between $1\,\mu m$ and $1\,cm$ at monterey bay determined using multiple instruments, Deep-Sea Res. I, 44, 1739–1767, 1997.

Jackson, G. A. and Burd, A. B.: A model for the distribution of particle flux in the mid-water column controlled by subsurface biotic interactions, Deep-Sea Res. II, 49, 193–217, 2002.

Khelifa, A. and Hill, P. S.: Models for effective density and settling velocity of flocs, J. Hydraul. Res., 44, 390–401, 2006a.

Khelifa, A. and Hill, P. S.: Kinematic assessment of floc formation using a monte carlo model, J. Hydraul. Res., 44, 548–559, 2006b.

Longhurst, A.: Seasonal cycles of pelagic production and consumption, Prog. Oceanogr., 36, 77–167, 1995.

Longhurst, A. R., Bedo, A. W., Harrison, W. G., Head, E. J. H., and Sameoto, D. D.: Vertical flux of respiratory carbon by oceanic diel migrant biota, Deep-Sea Res. A, 37, 685–694, 1990.

Lutz, M., Dunbar, R., and Caldeira, K.: Regional variability in the vertical flux of particulate organic carbon in the ocean interior, Global Biochem. Cycles, 16, 1–15, 2002.

Martin, J. H., Knauer, G. A., Karl, D. M., and Broenkow, W. W.: Vertex: Carbon cycling in the northeast pacific, Deep-Sea Res., 34, 267–285, 1987.

Martinez, E. and Maamaatuaiahutapu, K.: Island mass effect in the marquesas islands: Time

Aggregates distribution in the South-Eastern Pacific

L. Guidi et al.

variation, Geophys. Res. Lett., 31, L18307, doi:10.1029/2004GL020682, 2004.

McCave, I. N.: Vertical flux of particles in the ocean, Deep-Sea Res., 22, 491–502, 1975.

Michaels, A. F. and Silver, M. W.: Primary production, sinking fluxes and the microbial food web, Deep-Sea Res. A, 35, 473–490, 1988.

5 Morel, A., Gentili, B., Claustre, H., Babin, M., Bricaud, A., Ras, J., and Tieche, F.: Optical properties of the "Clearest" Natural waters, Limnol. Oceanogr., 52, 217–229, 2007.

Nodder, S. D., Duineveld, G. C. A., Pilditch, C. A., Sutton, P. J., Probert, P. K., Lavaleye, M. S. S., Witbaard, R., Chang, F. H., Hall, J. A., and Richardson, K. M.: Focusing of phytodetritus deposition beneath a deep-ocean front, Chatham rise, new Zealand, Limnol. Oceanogr., 52,

10 299–314, 2007.

Noji, T. T., Bathmann, U. V., vonBodungen, B., Voss, M., Antia, A., Krumbholz, M., Klein, B., Peeken, I., Noji, C. I. M., and Rey, F.: Clearance of picoplankton-sized particles and formation of rapidly sinking aggregates by the pteropod, limacina retroversa, J. Plankton Res., 19, 863–875, 1997.

15 Raimbault, P., Garcia, N., and Cerutti F.: Distribution of inorganic and organic nutrients in the South Pacific Ocean – evidence for long-term accumulation of organic matter in nitrogen-depleted waters, Biogeosciences Discuss., 4, 3041–3087, 2007,
http://www.biogeosciences-discuss.net/4/3041/2007/.

Ras, J., Claustre, H., and Uitz, J.: Spatial variability of phytoplankton pigment distributions

20 in the Subtropical South Pacific Ocean: comparison between in situ and predicted data, Biogeosciences Discuss., 4, 3409–3451, 2007,
http://www.biogeosciences-discuss.net/4/3409/2007/.

Richardson, T. L. and Jackson, G. A.: Small phytoplankton and carbon export from the surface ocean, Science, 315, 838–840, 2007.

25 Sarmiento, J. L. and Gruber, N.: Ocean Biogeochemical Dynamics, Princeton, Woodstock: Princeton University Press, 503 pp., 2006.

Steinberg, D. K., Van Mooy, B. A. S., Buesseler, K. O., Boyd, P. W., Kobari, T., and Karl, D. M.: Microbial vs. zooplankton control of sinking particle flux in the ocean's twilight zone, Limnol. Oceanogr., in press, 2008.

30 Stemmann, L., Gorsky, G., Marty, J. C., Picheral, M., and Miquel, J. C.: Four-year study of large-particle vertical distribution (0–1000 m) in the nw mediterranean in relation to hydrology, phytoplankton, and vertical flux, Deep-Sea Res. II, 49, 2143–2162, 2002.

Stemmann, L., Eloire, D., Sciandra, A., Jackson, G. A., Guidi, L., Picheral, M., and Gorsky, G.:

Volume distribution for particles between 3.5 to 2000 μm in the upper 200 m region of the South Pacific Gyre, Biogeosciences Discuss., 4, 3377–3407, 2007, http://www.biogeosciences-discuss.net/4/3377/2007/.

Suess, E.: Particulate organic-carbon flux in the oceans – surface productivity and oxygen utilization, Nature, 288, 260–263, 1980.

Thomas, A. C.: Seasonal distributions of satellite-measured phytoplankton pigment concentration along the chilean coast, J. Geophys. Res.-Oceans., 104, 25 877–25 890, 1999.

Volk, T. and Hoffert, M. I.: Ocean carbon pumps: Analysis of relative strengths and efficiencies in ocean-driven atmospheric co2 changes, in: The carbon cycle and atmospheric co2: Natural variations archean to present, American Geophysical Union ed., edited by: Sundquist, E. T. and Broecker, W. S., Geophysical monograph, Washington, D.C, 99–110, 1985.

Yu, E. F., Francois, R., Bacon, M. P., Honjo, S., Fleer, A. P., Manganini, S. J., van der Loeff, M. M. R., and Ittekot, V.: Trapping efficiency of bottom-tethered sediment traps estimated from the intercepted fluxes of th-230 and pa-231, Deep-Sea Res. I, 48, 865–889, 2001.

Aggregates distribution in the South-Eastern Pacific

L. Guidi et al.

Title Page

Abstract	Introduction
Conclusions	References
Tables	Figures

|◄ | ►|

◄ | ►

Back | Close

Full Screen / Esc

Printer-friendly Version

Interactive Discussion

EGU

Table 1. Location and time of the UVP deployments.

Station	Longitude	Latitude	Date	Time (UT)	Station	Longitude	Latitude	Date	Time (UT)
ES01	−144.001	−12.5	25-Oct-04	01:23 a.m.	STA13	−101.5	−29.09	22-Nov-04	11:31 a.m
MAR01	−141.14	−8.25	26-Oct-04	01:24 p.m.	STA15	−95.501	−30.42	24-Nov-04	11:34 a.m.
MAR02	−141.16	−8.23	27-Oct-04	10:32 a.m.	STA16	−92.59	−31.25	25-Nov-04	10:18 a.m.
MAR02	−141.16	−8.23	27-Oct-04	11:06 a.m.	EGY02	−91.28	−31.49	26-Nov-04	06:45 a.m.
MAR02	−141.16	−8.22	28-Oct-04	01:45 a.m.	EGY02	−91.27	−31.5	27-Nov-04	03:07 a.m.
MAR02	−141.16	−8.22	28-Oct-04	02:19 a.m.	EGY03	−91.25	−31.52	27-Nov-04	06:07 a.m.
MAR03	−141.16	−8.201	28-Oct-04	10:53 a.m.	EGY03	−91.25	−31.52	27-Nov-04	06:41 a.m.
MAR03	−141.16	−8.201	28-Oct-04	11:27 a.m.	EGY03	−91.24	−31.52	27-Nov-04	07:08 p.m.
MAR04	−141.16	−8.19	29-Oct-04	10:06 a.m.	EGY03	−91.24	−31.52	27-Nov-04	09:05 p.m.
MAR04	−141.16	−8.19	29-Oct-04	10:40 a.m.	EGY03	−91.24	−31.52	27-Nov-04	09:39 p.m.
HLNC01	−136.52	−9.001	31-Oct-04	12:57 p.m.	EGY04	−91.25	−31.52	28-Nov-04	08:54 a.m.
HLNC01	−136.52	−9.01	01-Nov-04	01:25 a.m.	EGY04	−91.25	−31.52	28-Nov-04	09:11 p.m.
HLNC02	−136.53	−9.001	01-Nov-04	10:14 a.m.	EGY04	−91.25	−31.52	28-Nov-04	09:45 p.m.
HLNC02	−136.53	−9.001	01-Nov-04	10:48 a.m.	EGY05	−91.25	−31.54	29-Nov-04	06:18 a.m.
HLNC02	−136.59	−9.03	02-Nov-04	05:09 a.m.	EGY05	−91.25	−31.54	29-Nov-04	06:52 a.m.
HLNC03	−136.58	−9.04	02-Nov-04	10:15 a.m.	EGY05	−91.21	−31.54	29-Nov-04	12:03 p.m.
HLNC03	−136.58	−9.04	02-Nov-04	10:49 a.m.	EGY05	−91.22	−31.53	29-Nov-04	09:49 p.m.
STA01	−134.21	−11.31	03-Nov-04	02:12 p.m.	EGY06	−91.24	−31.54	30-Nov-04	09:07 a.m.
STA03	−130.23	−15.08	05-Nov-04	01:39 p.m.	STA17	−87.26	−32.18	01-Dec-04	10:31 a.m.
STA05	−125.57	−18.301	07-Nov-04	01:36 p.m.	STA18	−84.04	−31.42	02-Dec-04	08:40 p.m.
STA07	−120.51	−21.44	09-Nov-04	01:05 p.m.	STA19	−81.38	−32.57	03-Dec-04	10:25 a.m.
STA09	−116.01	−24.42	11-Nov-04	12:51 p.m.	STA20	−78.22	−33.19	04-Dec-04	10:21 a.m.
GYRE02	−113.59	−26.001	12-Nov-04	11:56 a.m.	STA21	−75.501	−33.35	05-Dec-04	09:57 a.m.
GYRE03	−114.01	−26.001	13-Nov-04	08:16 a.m.	UPW01	−73.23	−33.52	07-Dec-04	01:27 a.m.
GYRE03	−114.01	−26.001	13-Nov-04	08:50 a.m.	UPW02	−73.23	−33.58	07-Dec-04	05:12 a.m.
GYRE03	−114.001	−26.03	13-Nov-04	11:19 p.m.	UPW02	−73.23	−33.58	07-Dec-04	05:46 a.m.
GYRE03	−114.001	−26.03	13-Nov-04	11:53 p.m.	UPW02	−73.24	−33.58	07-Dec-04	08:08 a.m.
GYRE04	−114.02	−26.04	14-Nov-04	10:53 a.m.	UPW02	−73.21	−33.52	07-Dec-04	09:21 p.m.
GYRE04	−114.02	−26.04	14-Nov-04	11:27 a.m.	UPW02	−73.21	−33.52	07-Dec-04	09:55 p.m.
GYRE04	−114.01	−26.05	14-Nov-04	11:20 p.m.	UPW03	−73.18	−33.5	08-Dec-04	06:26 a.m.
GYRE04	−114.01	−26.05	14-Nov-04	11:54 p.m.	UPW03	−73.18	−33.5	08-Dec-04	07:00 a.m.
GYRE05	−114.01	−26.04	15-Nov-04	08:08 a.m.	UPX01	−72.24	−34.32	09-Dec-04	09:03 p.m.
GYRE05	−114.01	−26.04	15-Nov-04	08:42 a.m.	UPX02	−72.26	−34.36	10-Dec-04	01:30 a.m.
GYRE05	−114.01	−26.04	15-Nov-04	09:16 a.m.	UPX02	−72.27	−34.37	10-Dec-04	06:29 a.m.
GYRE05	−114.02	−26.04	15-Nov-04	11:25 p.m.	UPX02	−72.27	−34.37	10-Dec-04	07:03 a.m.
GYRE06	−114.001	−26.04	16-Nov-04	10:28 a.m.	UPX02	−72.301	−34.401	11-Dec-04	01:21 a.m.
STA10	−110.401	−26.51	17-Nov-04	12:22 p.m.	UPX03	−72.29	−34.39	11-Dec-04	08:10 a.m.
STA11	−107.35	−27.42	20-Nov-04	12:17 p.m.	UPX03	−72.29	−34.39	11-Dec-04	08:39 a.m.

Aggregates distribution in the South-Eastern Pacific

L. Guidi et al.

Title Page

Abstract Introduction

Conclusions References

Tables Figures

◀◀ ▶▶

◀ ▶

Back Close

Full Screen / Esc

Printer-friendly Version

Interactive Discussion

EGU
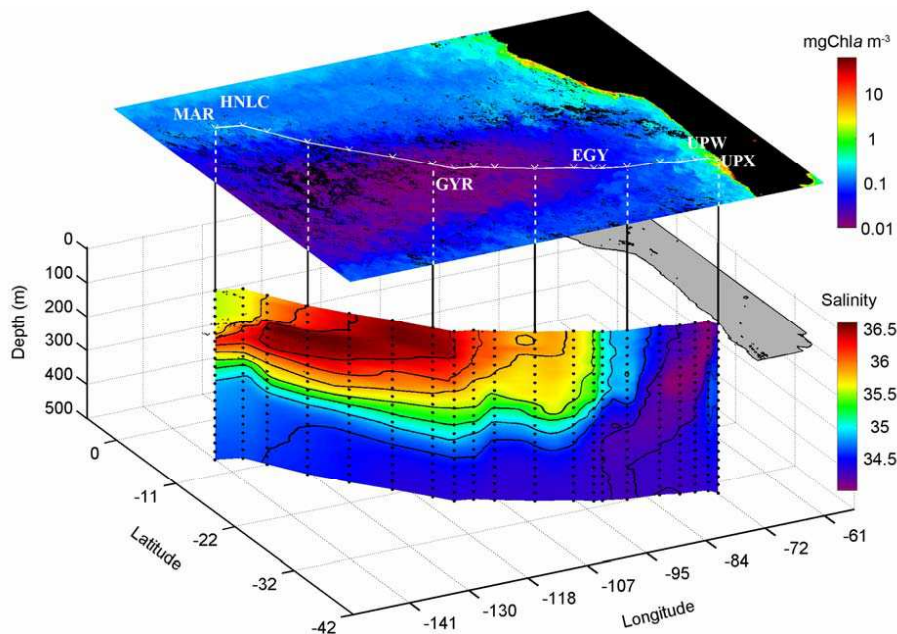
Fig. 1. Salinity section below the BIOSOPE transect superimposed on a SeaWiFS composite image of Chl*a* concentration. The South American continent is in black and grey. Position of the 6 long-term stations is from left to right: MAR – Marquesas station, HNLC, GYR, EGY, UPW and UPX stations.

EGU
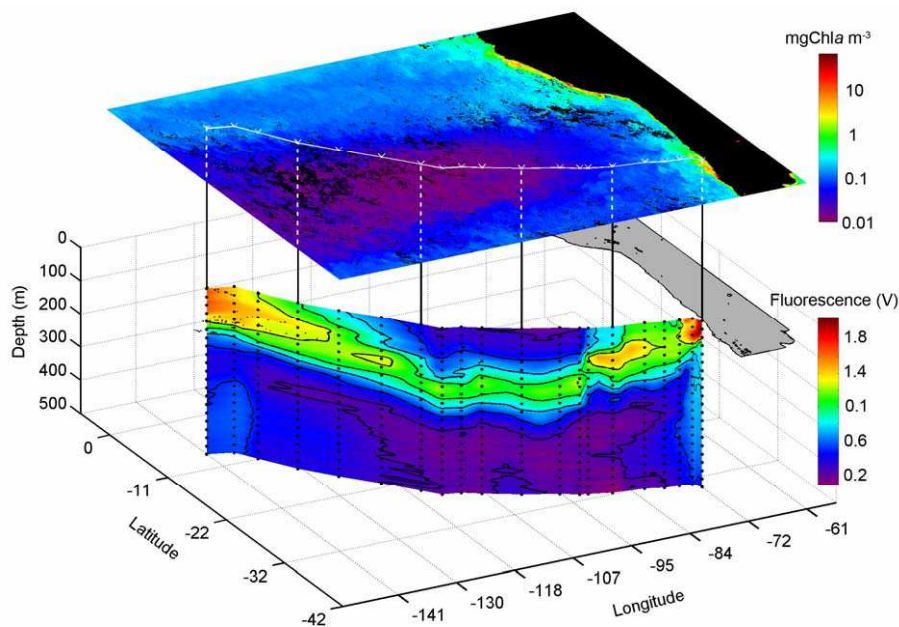
Fig. 2. In vivo fluorescence plot of Chl*a* along the BIOSOPE section. Note the relatively high values at each end of the transect.

EGU
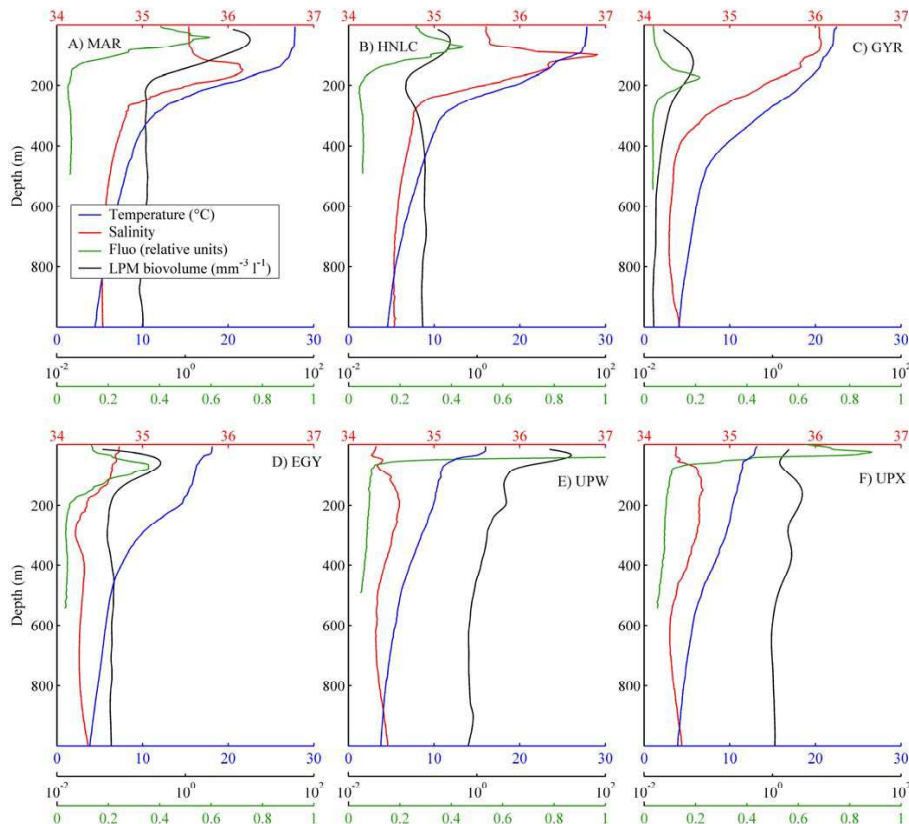
Fig. 3. Mean 0–1000 m profiles of the long-term stations displaying the temperature, salinity, fluorescence (RU) and the biovolumes (in mm^{-3} L^{-1}) of the LPM estimated from the UVP data. Note the logarithmic scale for the LPM data.

EGU

EGU
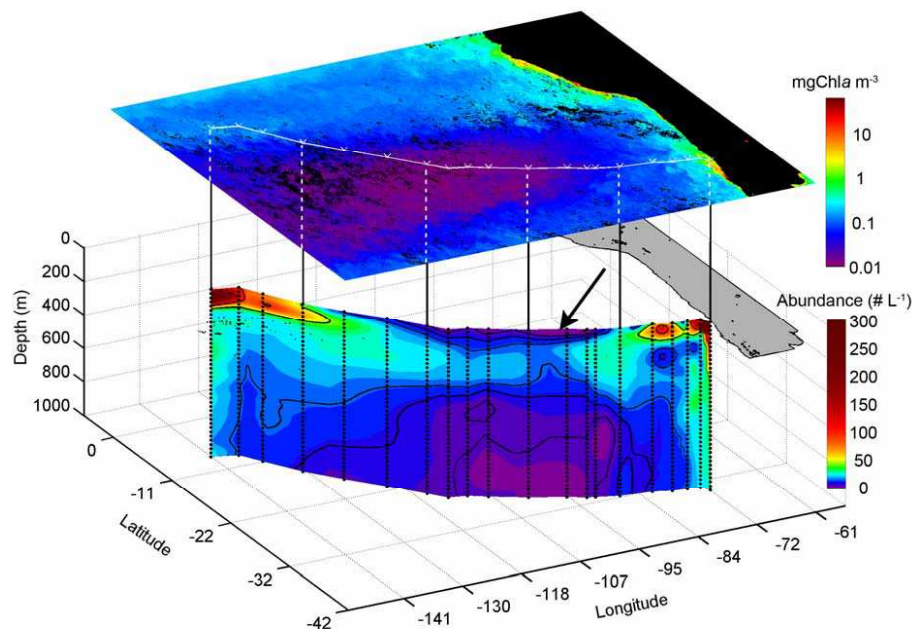
Fig. 4. Abundance of LPM $>100\,\mu$m in the first km of the BIOSOPE cruise. The arrow illustrate the discontinuity zone in the abundance distribution of the large particulate matter.
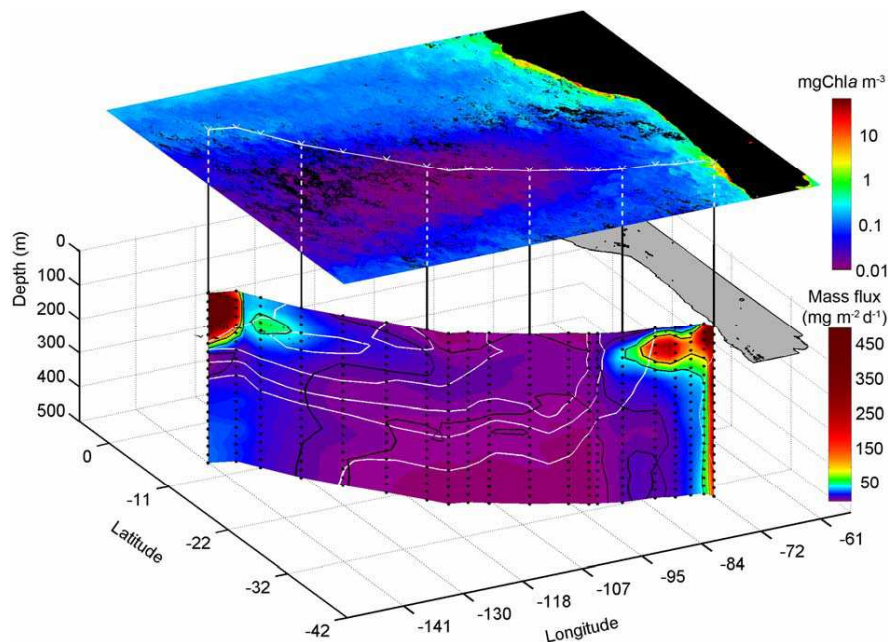
Fig. 5. Mass flux of LPM in mg DW m^{-2} d^{-1} estimated from size measurements of every individual particle recorded during the vertical deployment of the UVP. Only data from 0–500 m are shown for better visualisation of the superficial structures. The vertical resolution of the sampling was 10.5 L every 8 cm (see Guidi et al., 2007, for details). Isohalines are in white.
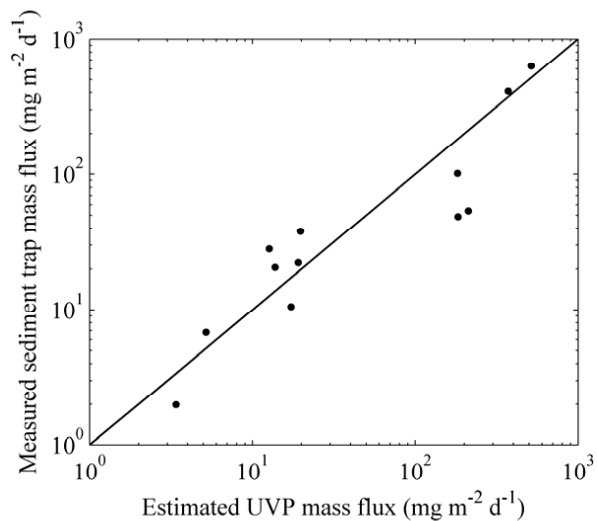
Fig. 6. Drifting sediment trap mass flux measurements versus the UVP estimated mass flux. The sediment traps were deployed below the mixed layer 200 m deep at the extremities of the transect and at the depth of about 400 m at the center of the SPG.

EGU
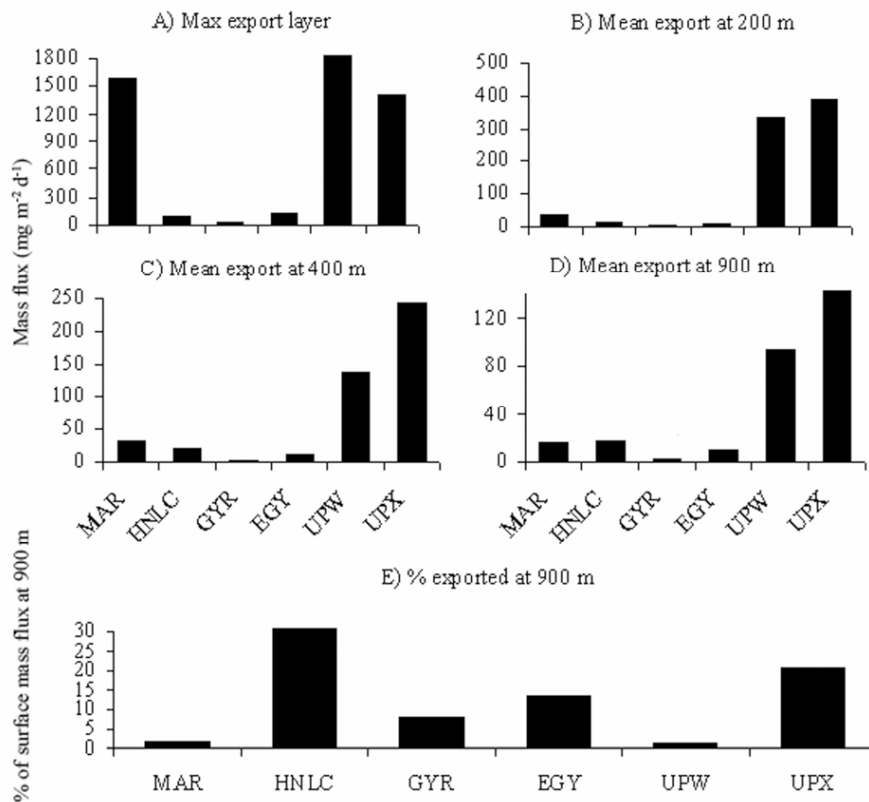
Fig. 7. Mean export at different depths and the % exported below 900 m related to the potential superficial export maximum.

EGU
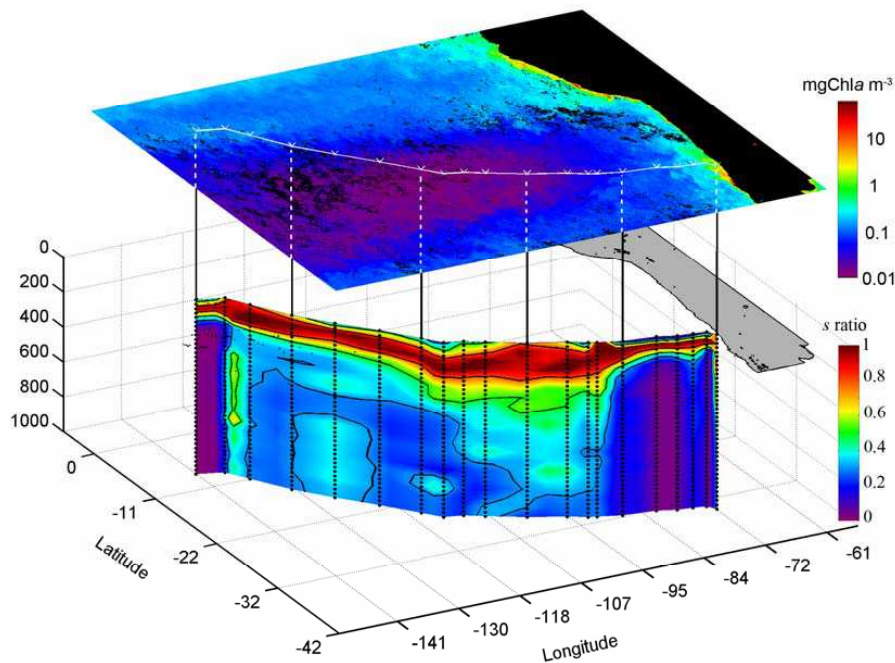
Fig. 8. The *s ratio* corresponding to the LPM mass flux (*F*) estimated at depth *Z* normalized by the flux estimated below Z_e (*s ratio*(*Z*)=*F*(*Z*)/*F*(Z_e)). Here, Z_e is the depth where the mass flux is maximal (*s ratio* is equal to 1 for Z_e: dark red).